The Importance of Measurement Errors for Deriving Accurate Reference Leaf Area Index Maps for Validation of Moderate-Resolution Satellite LAI Products

Dong Huang, Wenze Yang, Bin Tan, Miina Rautiainen, Ping Zhang, Jiannan Hu, Nikolay V. Shabanov, Sune Linder, Yuri Knyazikhin, and Ranga B. Myneni

***Abstract*—The validation of moderate-resolution satellite leaf area index (LAI) products such as those operationally generated from the Moderate Resolution Imaging Spectroradiometer (MODIS) sensor data requires reference LAI maps developed from field LAI measurements and fine-resolution satellite data. Errors in field measurements and satellite data determine the accuracy of the reference LAI maps. This paper describes a method by which reference maps of known accuracy can be generated with knowledge of errors in fine-resolution satellite data. The method is demonstrated with data from an international field campaign in a boreal coniferous forest in northern Sweden, and Enhanced Thematic Mapper Plus images. The reference LAI map thus generated is used to assess modifications to the MODIS LAI/fPAR algorithm recently implemented to derive the next generation of the MODIS LAI/fPAR product for this important biome type.**

***Index Terms*—Leaf area index (LAI), Moderate Resolution-Imaging Spectroradiometer (MODIS), validation of satellite biophysical products.**

I. Introduction

THE LAND team of the Moderate Resolution Imaging Spectroradiometer (MODIS) instruments aboard the National Aeronautics and Space Administration's Terra and Aqua satellites is responsible for the development of algorithms and validation of various biophysical data products operationally generated from the sensor data. The products include vegetation leaf area index (LAI) and fraction of photosynthetically active radiation (400–700 nm) absorbed by vegetation (fPAR) [1]. LAI and fPAR are used in climate modeling to describe the exchange of fluxes of energy, mass (e.g., water and CO_2), and momentum between the surface and the planetary boundary layer [2].

The validation of these biophysical products is presently a critical aspect of MODIS research. These activities are a key source of information to users on product accuracy and also serve as the basis for further algorithm and product refinement research. Product validation refers to assessment of product accuracy through comparisons to ground measurements that are scaled to MODIS resolution [3]. A direct comparison between sparsely sampled point field measurements and corresponding moderate-resolution satellite products (1 km) is not feasible because of scale-mismatch, geolocation errors, and land surface heterogeneity. Therefore, an intermediate step which involves scaling of field measurements to the resolution of satellite sensor products is required.

In the case of LAI validation, the spatial scaling is accomplished through the generation of a fine-resolution (20–30 m) map of an area covering several moderate-resolution pixels, typically 10 km $\times$ 10 km. This reference LAI map is derived from correlations between field measurements and fine-resolution satellite reflectance data over a smaller area (1 km $\times$ 1 km or 3 km $\times$ 3 km) within this large region [4]–[6]. The fine-resolution LAI map when aggregated to the resolution of the MODIS product serves as the benchmark. Therefore, it is important to characterize the accuracy of the benchmark itself in order to have confidence in the validation procedure, and this is the theme of this paper.

An accurate site-specific relationship between field-measured LAI and fine-resolution satellite reflectance data must be established in order to generate the reference LAI map. A small perturbation in either of these data is likely to alter the relationship. These perturbations can arise in many ways. For example, LAI values at the validation site are derived from measurements of downward radiation fluxes measured below the vegetation canopy. The equations at the heart of this derivation are based on certain assumptions about the spatial and angular distribution of canopy elements that are often not met in reality. Further, the precision of field measurements, especially in case of sparse vegetation canopies, can be low because of spatial heterogeneity. Likewise, the fine-resolution surface reflectance data have a certain accuracy and precision caused by incomplete atmospheric correction, calibration and geolocation errors, etc. Thus, errors in both field and satellite measurements must be accounted in order to derive an unbiased site-specific relationship [5], [7].

The objective of this paper is to develop a simple method that accounts for measurement errors in the generation of a

Manuscript received November 1, 2004; revised January 24, 2006. This work was supported by the National Aeronautics and Space Administration under MODIS Contracts NAS5-96061 and NNG04HZ09C.

D. Huang, W. Yang, B. Tan, P. Zhang, J. Hu, N. V. Shabanov, Y. Knyazikhin, and R. B. Myneni are with the Department of Geography, Boston University, Boston, MA 02215 USA (e-mail: dh@bu.edu).

M. Rautiainen is with the Department of Forest Ecology, University of Helsinki, Helsinki FI-00014, Finland.

S. Linder is with the Swedish University of Agricultural Sciences, SE-230 53 Alnarp, Sweden.

Digital Object Identifier 10.1109/TGRS.2006.876025

fine-resolution reference LAI map. The method will be demonstrated with data from an international field campaign in a boreal coniferous forest in northern Sweden, and Enhanced Thematic Mapper Plus (ETM+) images. The reference LAI map thus generated will be used to assess modifications to the MODIS LAI/fPAR algorithm recently implemented to derive the next generation of the MODIS LAI/fPAR product for this important biome type.

II. Methods

The simple linear regression model has the form $Y = \alpha + \beta X + u(Y)$ where α and β are the coefficients of the regression line and u represents measurement errors in Y. We assume that u has zero mean, constant variance, and zero covariances. The coefficients α and β can be estimated by the method of ordinary least square (OLS) through minimization of the Euclidean distance $\|Y - \hat{Y}\|$ between vectors of observed Y and predicted $\hat{Y}$ variables. Errors in measurements of the dependent variable Y do not bias the estimated relationship but can result in poor precision of the estimator β [8]. It is generally assumed that the vector X of observed independent variables is free of any measurement errors, and that measurement errors in Y are independent of X. If there are measurement errors in the independent variable, i.e., $X = \widetilde{X} + v(\widetilde{X})$, and the measurement error in Y is uncorrelated with both the true values and the measurement errors of the independent variable, the estimate $\hat{\beta}$ of β will be biased [7]–[9], i.e.,

$$\hat{\beta} = \frac{\mathrm{cov}(X,Y)}{\sigma_X^2} = \frac{\beta}{1 + \frac{\sigma_v^2}{\sigma_{\widetilde{X}}^2}}. \tag{1}$$

Here σ_X^2 is the variance of X; $\sigma_v^2 < \infty$ denotes the variance of the measurement error in the dependent variable; and $\sigma_{\widetilde{X}}^2$ is the variance of true $\widetilde{X}$ values. The measurement error and true values are assumed to be uncorrelated. The coefficient σ_v is called measurement precision in remote sensing [5].

Thus, any measurement error in X will result in a bias in the coefficient β. If β is positive in the relationship between field-measured LAI (Y) and fine-resolution satellite reflectance data (X), the LAI values above the mean will be underestimated and overestimated below the mean [7]. Any reference or benchmark LAI maps generated with regression models that do not account for measurement errors will not serve the purpose of validation of moderate-resolution sensor products, especially the MODIS LAI/fPAR products because the corresponding algorithm explicitly accounts for errors in input surface reflectances [10], [11].

Information on measurement errors can help to improve estimates of β [12]–[14]. If measurement errors in X and Y are uncorrelated, then $\sigma_{\widetilde{X}}^2 = \sigma_X^2 - \sigma_v^2$ and the true regression coefficient β takes the following form [7]:

$$\beta = \frac{\mathrm{cov}(X,Y)}{\sigma_X^2 - \sigma_v^2}. \tag{2}$$

Thus, the regression coefficient $\hat{\beta}$ derived directly from measurements using the OLS method should be multiplied by $h = \beta/\hat{\beta}$ to obtain the unbiased estimate. It follows from (1) and (2) that

$$h = \frac{\sigma_X^2}{\sigma_X^2 - \sigma_v^2}. \tag{3}$$

The measurement precision σ_v of reflectance data can be evaluated with data from invariant targets. Successive and repetitive reflectance measurements of these surfaces may be used to characterize the mean, variance, and precision, for we can expect minimal changes in the reflectance of an invariant surface if the instrument and the atmospheric correction are stable. The average relative precision (precision divided by mean) of the MODIS surface reflectance product for an invariant vegetated surface was estimated to be about 13% to 15% at the red and near-infrared (NIR) wavelength [15]. We will use this information to estimate the correction coefficient h.

Let $\delta_{\max}$ be the upper limit of relative precision in satellite reflectance data. We shall assume the relative errors to be distributed in the interval between $-\delta_{\max}$ and $+\delta_{\max}$. Thus, the remotely sensed variable X can be approximated as $X = \widetilde{X} + \widetilde{X}\delta_{\max}\xi$ where ξ is a random variable distributed between -1 and 1 which has zero expectation, $E\xi = 0$, and a finite variance $E\xi^2 = \sigma_0^2$. If the observed variable and its error are independent then

$$\begin{aligned}\sigma_v^2 &= E(\widetilde{X}\delta_{\max}\xi)^2 = \delta_{\max}^2 E(\widetilde{X}^2) E\xi^2 \\ &= \delta_{\max}^2\sigma_0^2 E\left(\widetilde{X}^2 - (E\widetilde{X})^2 + (E\widetilde{X})^2\right) \\ &= \delta_{\max}^2\sigma_0^2\left[\sigma_{\widetilde{X}}^2 + (E\widetilde{X})^2\right] \\ &= \delta_{\max}^2\sigma_0^2\left[\sigma_X^2 - \sigma_v^2 + (E\widetilde{X})^2\right].\end{aligned} \tag{4}$$

Resolving this equation for σ_v^2 one gets

$$\sigma_v^2 = \frac{\sigma_0^2\delta_{\max}^2\left[\sigma_X^2 + (E\widetilde{X})^2\right]}{1 + \sigma_0^2\delta_{\max}^2}. \tag{5}$$

Substituting this equation into (3) results in

$$h = 1 + \frac{\sigma_0^2\delta_{\max}^2\left(\delta_X^2 + 1\right)}{\delta_X^2 - \sigma_0^2\delta_{\max}^2} \tag{6}$$

where $\delta_X = \sigma_X/EX$ is the coefficient of variation of X. This equation will be used to correct the estimate $\hat{\beta}$. The intercept $\hat{\alpha}$ of the linear regression model is given as $\hat{\alpha} = EY - h\hat{\beta}EX$.

III. Reference LAI Map and MODIS LAI Product

A. Data Used

The Flakaliden field campaign was conducted between June 25 and July 4, 2002 with the objective of collecting data needed for validation of two MODIS products for needle forests—LAI and fraction of photosynthetically active radiation (fPAR) absorbed by the vegetation canopy. There were 39 participants from seven countries: Sweden, Finland, U.S., Italy, Germany, Estonia, and Iceland. The Flakaliden is located in northern Sweden, a region dominated by boreal forests. Leaf area index data were collected at three forested sites (Fig. 1) located near the town of Vindeln, with operations based at the Flakaliden site. The sites were chosen to represent different types of boreal

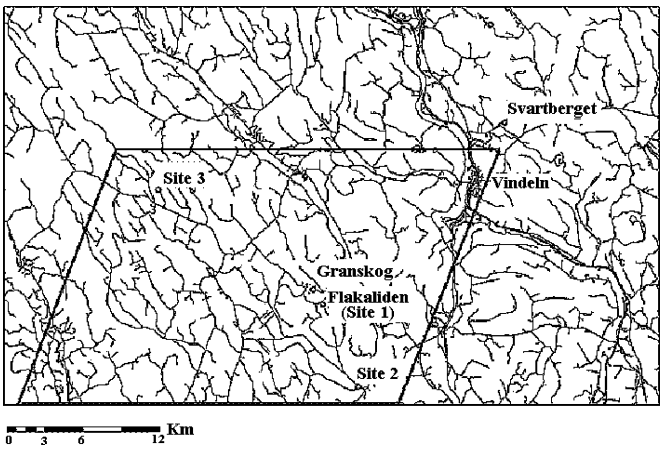

Fig. 1. Forested sites where LAI data were collected. These sites are located near the town of Vindeln, Sweden, with operations based at Flakaliden, a long-term research site which has been operational since 1987 [16]. The 30 km × 30 km area for which the reference LAI map was produced is shown as a parallelogram. This figure is by courtesy of Matt Jolly.

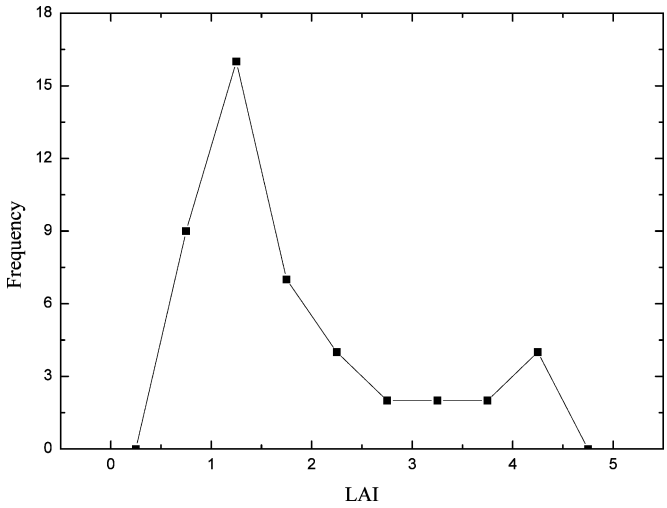

Fig. 2. Histogram of LAI values collected at three forest sites. Mean LAI is 1.83. STD is 1.04.

forests, both homogeneous and mixed Norway spruce and Scots pine stands. The sites are described in some detail below.

Flakaliden Research Area (Site 1): LAI data were collected in six plots of planted 40-year-old Norway spruce (*Picea Abies (L.) Karst*). Each plot is a 50 m × 50 m area. Measurements were made on a six by three grid set up in the center of the plot. Four of the plots had been subjected to nutrient optimization since 1987. The long-term nutrient treatment had resulted in drastic effects on stand structure and production [16]. Global positioning system (GPS) coordinates were also recorded. The mean LAI of the six plots is 3.64 (STD = 0.9).

Site 2: This site represents a uniform pine stand composed of Scots pine (*Pinus Sylvestris*). A 100 m × 100 m plot within the stand was chosen for sampling. Leaf area index and GPS measurements were collected on a 20 m × 20 m grid point corners within this plot. The mean LAI and STD for this site are 0.98 and 0.05, respectively.

Site 3: This site is a 1 km × 1 km mixed needle leaf forest stand typical of the vegetation in a 200 km × 200 km area around Flakaliden. The site was divided into four 1-km east-to-west transects spaced about 250 m apart. Leaf area index and GPS measurements were made at every 10 to 20 m along these transects. The mean LAI and STD are 1.87 and 0.6, respectively. Fig. 2 shows a histogram of LAI values collected at the three sites.

Leaf area index was measured with a LAI-2000 plant canopy analyzer. Readings were taken using a 45° restrictor. LAI values were calculated according to Miller's derivation [17], which is the default method used by LAI-2000. These values are estimates of effective leaf area index. The MODIS LAI product in the case of needle canopies is also effective leaf area index because the algorithm considers shoots as the basic foliage elements and retrieves shoot silhouette area index [18]–[20]. It should be noted that the default method converts canopy gap fraction into LAI under the assumption of uniformly distributed foliage elements and, moreover, the LAI-2000 cannot distinguish between foliage and woody material. This can cause biases in relationships between MODIS and field effective LAIs.

A cloud-free Landsat ETM+ image from August 20, 2002 was registered to the ground sampling points using aerial photographs with accurate coordinates. The ETM+ digital counts were converted to reflectance by the dark object subtraction method [21]. Data from bands 3 (red, 630–690 nm), 4 (NIR, 780–900 nm), and 5 [shortwave infrared (SWIR), 1550–1750 nm] were used in this study. There were 46 ETM+ pixels within which field LAI measurements were taken. The average of local LAI values is assumed to be the LAI of the corresponding ETM+ pixel.

B. Linear Regression Model

The reduced simple ratio (RSR) [22] is used to derive a linear regression model

$$\mathrm{RSR} = \frac{\rho_{\mathrm{NIR}}}{\rho_{\mathrm{red}}}\left[1 - \frac{\rho_{\mathrm{SWIR}} - \min(\rho_{\mathrm{SWIR}})}{\max(\rho_{\mathrm{SWIR}}) - \min(\rho_{\mathrm{SWIR}})}\right] \quad (7)$$

where ρ_{red}, ρ_{NIR}, and ρ_{SWIR} are the red, NIR, and SWIR reflectances, respectively, and the $\min(\rho_{\mathrm{SWIR}})$ and $\max(\rho_{\mathrm{SWIR}})$ are the minimum and maximum SWIR reflectance found in the ETM+ image. Several studies suggested the use of SWIR reflectance and the RSR to account for the impact of understory reflectances [22].

If errors in spectral reflectances are independent, the relative error in the RSR can be obtained by differentiating (7) and neglecting second- and higher order terms

$$\begin{aligned}\delta_{\max} &= \left|\frac{\Delta \mathrm{RSR}}{\mathrm{RSR}}\right| = |\Delta \ln \mathrm{RSR}| \\ &= \left|\frac{\Delta\rho_{\mathrm{NIR}}}{\rho_{\mathrm{NIR}}} - \frac{\Delta\rho_{\mathrm{red}}}{\rho_{\mathrm{red}}} - \frac{\Delta\rho_{\mathrm{SWIR}}}{\max(\rho_{\mathrm{SWIR}}) - \rho_{\mathrm{SWIR}}}\right| \\ &\le \delta_{\mathrm{NIR}} + \delta_{\mathrm{red}} + \delta_{\mathrm{SWIR}} \end{aligned} \quad (8)$$

where δ_k, k = red, NIR, are relative errors in ETM+ surface reflectances, and δ_{SWIR} represents $|\Delta\rho_{\mathrm{SWIR}}|$ normalized by $\max(\rho_{\mathrm{SWIR}}) - \rho_{\mathrm{SWIR}}$. Although errors in ETM+ surface reflectance can be different than errors in MODIS data, we use em-

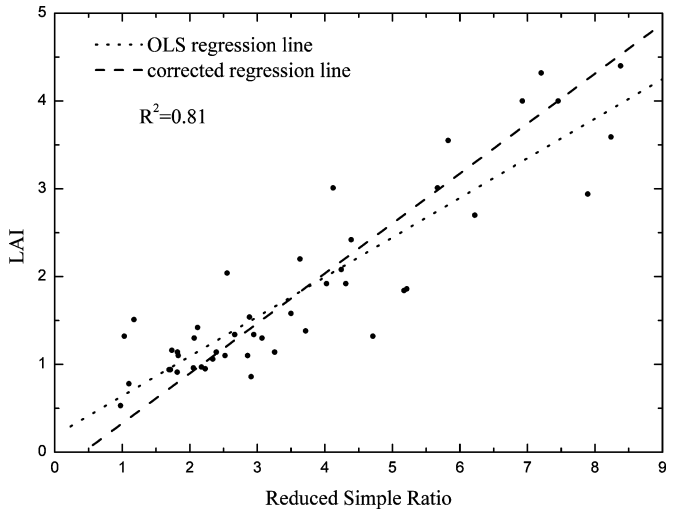

Fig. 3. Correlation between the RSR and LAI. The regression line obtained with the standard OLS method is LAI $= 0.45 \cdot$ RSR $+ 0.19$. The regression model changes to LAI $= 0.560 \cdot$ RSR $- 0.24$ after applying the correction procedure which accounts for measurements errors.

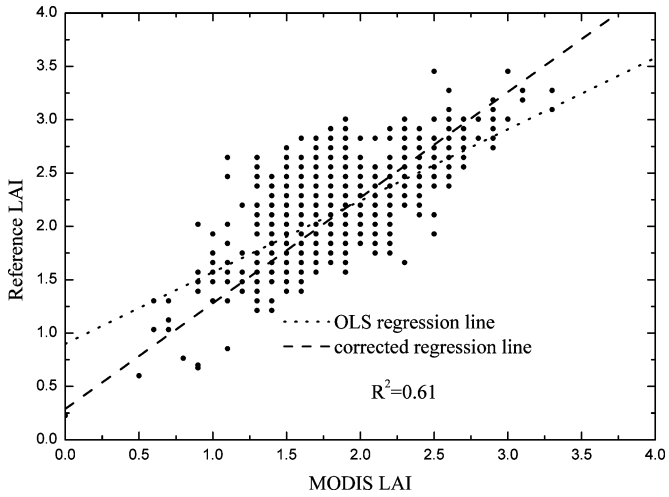

Fig. 4. Correlation between the reference and MODIS LAI values. The regression line obtained with the standard OLS method is $\mathrm{LAI_{ref}} = 0.67\mathrm{LAI_{MODIS}} + 0.9$. The regression model changes to $\mathrm{LAI_{ref}} = 0.99\mathrm{LAI_{MODIS}} + 0.29$ after applying the correction procedure which accounts for precision of the reference LAI values.

pirical estimates of the upper limit of the relative precision derived for the MODIS red and NIR spectral bands, $\delta_{\mathrm{red}} = 0.15$; $\delta_{\mathrm{NIR}} = 0.15$, [11] and a theoretical estimate for the MODIS SWIR band, $\delta_{\mathrm{SWIR}} = 0.10$ [11], [24]. Thus, the relative precision can be estimated from above as $\delta_{\max} \leq 0.15 + 0.15 + 0.10 = 0.40$. The coefficient of variation δ_X calculated for the 46 ETM+ pixels is 0.57. The correction factor h calculated from (6) takes the value 1.26. The variance σ_0^2 is set to 1/3, which corresponds to a uniformly distributed random variable ξ.

It should be noted that the above assumption about spectral independence of errors is not always true. In this case, information about interdependences of spectral reflectances is needed to evaluate the relative precision. Their interdependences are usually given by a system of nonlinear equations $f_k(\rho_1, \rho_2, \ldots, \rho_n) = 0$, $k \leq n$ which, in turn, determines a true value of $\delta_{\max}$. This information was not available at time of this research, and thus (8) was used to estimate the relative precision.

Fig. 3 shows variation in LAI with respect to the RSR. The regression of LAI with respect to the RSR with the OLS method is LAI $= 0.45 \cdot$ RSR $+ 0.19$. After applying the correction technique which accounts for errors in satellite observations, as described earlier, the linear regression model changes to LAI $= 0.60 \cdot$ RSR $- 0.24$. The R^2 is 0.81 in both cases.

C. Comparison of Reference and MODIS LAI Maps

A previous study on the validation of Collection 4 MODIS LAI product at a coniferous forest site in Finland found the product to be accurate to within 0.5 LAI but the precision to be much worse than expected [4]. This suggested a need for algorithm refinements. Several modifications have been implemented in the version of the algorithm slated for Collection 5 processing [25]. A prototype of the MODIS LAI product generated with this Collection 5 algorithm is tested here with data from the Flakaliden campaign. To this end, a 30 km $\times$ 30 km area near Flakaliden (Fig. 1) was selected as the test site for comparing the MODIS product to reference LAI values. There are two ways to generate such reference LAI values.

First, by regressing field-measured LAI and the corresponding ETM+-based RSR and using this regression model (Fig. 3—OLS regression line) to generate a 30-m resolution LAI map of the 30 km $\times$ 30 km study area. This fine-resolution map is then aggregated to 1-km resolution and compared to the corresponding MODIS product. The MODIS LAI will be taken as the independent variable when regressing its values and the reference map in our analyses since its precision is known. The regression line gives the best possible prediction of the "true LAI" given MODIS product. In this case, the resulting regression line is $\mathrm{LAI_{ref}} = 0.53 \cdot \mathrm{LAI_{MODIS}} + 1.2$, i.e., the MODIS LAI values overestimate "the true values" above the mean LAI and underestimates below the mean. This neither validates nor invalidates the MODIS product because the model used to generate the fine-resolution reference LAI map did not take into account errors in field LAI measurements and ETM+ surface reflectances.

Second, by regressing field-measured LAI and ETM+ based RSR using the correction technique which explicitly accounts for errors in satellite observations [see (6)] (Fig. 3—Corrected regression line). The resulting fine-resolution map of the 30 km $\times$ 30 km study area is then aggregated to 1-km resolution and compared to the corresponding MODIS LAI product (Fig. 4) without accounting for the precision of the MODIS product. The regression between the reference LAI and MODIS product is $\mathrm{LAI_{Ref}} = 0.67 \cdot \mathrm{LAI_{MODIS}} + 0.9$. Although a better correspondence is obtained, agreement between reference values and MODIS product is still poor. Again, this neither validates nor invalidates the MODIS product because this comparison does not take into account the precision of the MODIS LAI values.

The precision of the MODIS LAI product is about 0.2 [5], [15]. Taking this precision into account through the correction method developed in this paper, the resulting regression is

$\mathrm{LAI}_{\mathrm{ref}} = 0.99\mathrm{LAI}_{\mathrm{MODIS}} + 0.29$. This clearly shows much better comparability between the MODIS product and the reference values. Thus, it is important to account for both: 1) errors in fine-resolution satellite-based surface reflectances in building an empirical model for generating fine-resolution reference LAI maps and 2) precision of the moderate-resolution satellite sensor products, such as the MODIS LAI, when comparing the reference and retrieved values.

IV. Conclusion

Validation refers to assessment of a satellite sensor product's accuracy through comparisons to ground measurements. A direct comparison between sparsely sampled point field measurements and corresponding moderate-resolution satellite products (1 km) is not feasible because of scale-mismatch, geolocation errors, and land surface heterogeneity. Therefore, scaling of field measurements to the resolution of satellite sensor products is a key intermediate step in validation. In the case of LAI validation, the spatial scaling is accomplished through the generation of a fine-resolution (20–30 m) map of an area covering several moderation resolution pixels, typically 10 km $\times$ 10 km. This reference LAI map is derived from correlations between field measurements and fine-resolution satellite-measured reflectance data over a smaller area (1 km $\times$ 1 km or 3 km $\times$ 3 km) within this large region. The fine-resolution LAI map when aggregated to the resolution of the MODIS LAI product serves as the reference field. The analysis presented in this paper shows that it is important to account for both:1) errors in field measurements of LAI and fine-resolution satellite-based surface reflectances in building empirical models for generating fine-resolution reference LAI maps and 2) precision of the moderate-resolution satellite sensor product, such as the MODIS LAI, when comparing it to reference values.

Acknowledgment

The authors thank the participants of the Flakaliden field campaign for making the data available for this investigation.

References

[1] C. O. Justice, J. R. G. Townshend, E. F. Vermote, E. Masuoka, R. E. Wolfe, N. Saleous, D. P. Roy, and J. T. Morisette, "An overview of MODIS Land data processing and product status," *Remote Sens. Environ.*, vol. 83, pp. 3–15, 2002.

[2] P. J. Sellers, R. E. Dickinson, D. A. Randall, A. K. Betts, F. G. Hall, J. A. Berry, G. J. Collatz, A. S. Denning, H. A. Mooney, C. A. Nobre, N. Sato, C. B. Field, and A. Henderson-Sellers, "Modeling the exchanges of energy, water, and carbon between continents and the atmosphere," *Science*, vol. 275, pp. 502–509, 1997.

[3] J. T. Morisette, J. L. Privette, and C. O. Justice, "A framework for the validation of MODIS land products," *Remote Sens. Environ.*, vol. 83, pp. 77–96, 2002.

[4] Y. Wang, C. E. Woodcock, W. Buermann, P. Stenberg, P. Voipio, H. Smolander, T. Hame, Y. Tian, J. Hu, Y. Knyazikhin, and R. B. Myneni, "Evaluation of the MODIS LAI algorithm at a coniferous forest site in Finland," *Remote Sens. Environ.*, vol. 91, pp. 114–127, 2004.

[5] B. Tan, J. Hu, P. Zhang, D. Huang, N. Shabanov, M. Weiss, Y. Knyazikhin, and R. B. Myneni, "Validation of MODIS LAI product in croplands of Alpilles, France," *J. Geophys. Res.*, vol. 110, no. D01107, 2005. DOI: 10.1029/2004JD004860.

[6] W. B. Cohen, T. K. Maiersperger, Z. Yang, S. T. Gower, D. P. Turner, W. D. Ritts, M. Berterretche, and S. W. Running, "Comparisons of land cover and LAI estimates derived from ETM+ and MODIS for four sites in North America: A quality assessment of 2000/2001 provisional MODIS products," *Remote Sens. Environ.*, vol. 88, pp. 233–255, 2003.

[7] P. J. Curran and A. M. Hay, "The importance of measurement error for certain procedures in remote sensing at optical wavelengths," *Photogramm. Eng. Remote Sens.*, vol. 52, pp. 229–241, 1986.

[8] J. Hausman, "Mismeasured variables in econometric analysis: problems from the right and problems from the left," *J. Econ. Perspectives*, vol. 15, pp. 57–67, 2001.

[9] J. Johnston, *Econometric Methods*. New York: Wiley, 1992, pp. 281–284.

[10] Y. Knyazikhin, J. V. Martonchik, R. B. Myneni, D. J. Diner, and S. W. Runing, "Synergistic algorithm for estimating vegetation canopy leaf area index and fraction of absorbed photosynthetically active radiation from MODIS and MISR data," *J. Geophys. Res.*, vol. 103, pp. 32 257–32 275, 1998.

[11] Y. Wang, Y. Tian, Y. Zhang, N. El-Saleous, Y. Knyazikhin, E. Vermote, and R. B. Myneni, "Investigation of product accuracy as a function of input and model uncertainties: Case study with SeaWiFS and MODIS LAI/FPAR Algorithm," *Remote Sens. Environ.*, vol. 78, pp. 296–311, 2001.

[12] A. Madansky, "The fitting of straight lines when both variables are subjected to error," *Amer. Statist.*, vol. 54, pp. 173–205, 1959.

[13] P. Sprent, *Models in Regression and Related Topics*. London, U.K .: Methuen, 1969.

[14] R. Fernandes, C. Butson, S. Leblanc, and R. Latifovic, "Landsat-5 TM and Landsat-7 ETM+ based accuracy assessment of leaf area index products for Canada derived from SPOT-4 VEGETATION data," *Can. J. Remote Sens.*, vol. 29, no. 2, pp. 241–258, 2003.

[15] W. Yang, B. Tan, D. Huang, M. Rautiainen, N. Shabanov, Y. Wang, J. L. Privette, K. F. Huemmrich, R. Fensholt, I. Sandholt, M. Weiss, R. R. Nemani, Y. Knyazikhin, and R. B. Myneni, "MODIS leaf area index products: From validation to algorithm improvement," *IEEE Trans. Geosci. Remote Sens.*, vol. 44, no. 7, pp. 1885–1898, Jul. 2006.

[16] J. Bergh, S. Linder, T. Lundmark, and B. Elfving, "The effect of water and nutrient availability on the productivity of Norway spruce in northern and southern Sweden," *Forest Ecol. Manage.*, vol. 119, pp. 51–62, 1999.

[17] J. B. Miller, "A formula for average foliage density," *Aust. J. Bot.*, vol. 15, pp. 141–144, 1967.

[18] Y. Knyazikhin, G. Miessen, O. Panferov, and G. Gravenhorst, "Small-scale study of three-dimensional distribution of photosynthetically active radiation in a forest," *Agricult. Forest Meteorol.*, vol. 88, pp. 215–239, 1997.

[19] Y. Wang, W. Buermann, P. Stenberg, H. Smolander, T. Hame, Y. Tian, J. Hu, Y. Knyazikhin, and R. B. Myneni, "A new parameterization of canopy spectral response to incident solar radiation: Case study with hyperspectral data from pine dominant forest," *Remote Sens. Environ.*, vol. 85, pp. 304–315, 2003.

[20] S. Smolander and P. Stenberg, "A method to account for shoot scale clumping in coniferous canopy reflectance models," *Remote Sens. Environ.*, vol. 88, pp. 363–373, 2003.

[21] M. S. Moran, R. D. Jackson, P. N. Slater, and P. M. Teillet, "Evaluation of simplified procedures for retrieval of land surface reflectance factors from satellite sensor output," *Remote Sens. Environ.*, vol. 41, pp. 169–184, 1992.

[22] L. Brown, J. M. Chen, S. G. Leblanc, and J. Cihlar, "A shortwave infrared modification to the simple ratio for LAI retrieval in Boreal forests: An image and model analysis," *Remote Sens. Environ.*, vol. 71, pp. 16–25, 2000.

[23] J. M. Chen, G. Pavlic, L. Brown, J. Cihlar, S. G. Leblanc, H. P. White, R. J. Hall, D. R. Peddle, D. J. King, J. A. Trofymow, E. Swift, J. Van der Sanden, and P. K. E. Pellikka, "Derivation and validation of Canada-wide coarse-resolution leaf area index maps using high-resolution satellite imagery and ground measurements," *Remote Sens. Environ.*, vol. 80, pp. 165–184, 2002.

[24] E. Vermote, "Product accuracy/Uncertainty: MOD09, surface reflectance atmospheric correction algorithm product," Goddard Space Flight Center, Greenbelt, MD, 2000. MODIS Data Products Catalog (EOS AM Platform). [Online]. Available: http://modarch.gsfc.nasa.gov/MODIS/RESULTS/DATAPROD.

[25] N. V. Shabanov, S. Kotchenova, D. Huang, W. Yang, Y. Knyazikhin, and R. B. Myneni, "Analysis and optimization of the MODIS leaf area index algorithm retrievals over broadleaf forests," *IEEE Trans. Geosci. Remote Sens.*, vol. 43, no. 8, pp. 1855–1865, Aug. 2005.

Dong Huang received the B.S. degree in physics from Beijing Normal University, Beijing, China, in 1999. He is currently pursuing the Ph.D. degree at Boston University, Boston, MA.

His main competences and interests are in remote sensing of vegetation, radiative transfer, and parameterization of land surface radiation budget. He has made special contribution on the use of foliage spatial correlation in 3-D radiative transfer. His stochastic radiative transfer model, which has been demonstrated to be as simple as 1-D and as realistic as 3-D models, provides a powerful tool for vegetation remote sensing and climate modeling. He has also developed a novel and powerful parameterization for radiation partitioning on vegetated land surface using the concepts of spectral invariant.

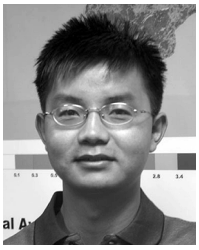

Wenze Yang received the B.S. and MS degrees in automation engineering from Tsinghua University, Beijing, China, and the Ph.D. degree in geography from Boston University, Boston, MA, in 1998, 2001, and 2006, respectively.

His research interest focuses on remote sensing on vegetation, diagnosis and evaluation of satellite-retrieved surface data, and climate–vegetation interactions.

Bin Tan, photograph and biography not available at the time of publication.

Miina Rautiainen received the Ph.D. degree in forestry from the University of Helsinki, Helsinki, Finland, in 2006.

She is is currently with the Department of Forest Ecology, University of Helsinki.

Ping Zhang received the B.S. and M.S. degrees in geography from Peking University, Beijing, China, in 1998 and 2001. She is currently pusuing the Ph.D. degree at Boston University, Boston, MA.

Her current research interests are climate impacts upon vegetation and agriculture, the use of remote sensing to monitor and predict famine, and climate–vegetation interactions and feedback related to seasonal climate variability.

Jiannan Hu, photograph and biography not available at the time of publication.

Nikolay V. Shabanov received the Ph.D. degree in remote sensing from Boston University, Boston, MA, in 2002.

He is currently a Research Assistant Professor in the Geography Department, Boston University, where his research includes parameterizing the effect of vegetation spatial heterogeneity with stochastic radiative transfer theory and development of algorithms for retrieving biophysical parameters from satellite data.

Sune Linder, photograph and biography not available at the time of publication.

Yuri Knyazikhin, photograph and biography not available at the time of publication.

Ranga B. Myneni received the Ph.D. degree in biology from the University of Antwerp, Antwerp, Belgium, in 1985.

He is currently a Professor and Faculty member in the Department of Geography, Boston University, Boston, MA, where his research interests are in radiative transfer, remote sensing of vegetation, and climate–vegetation dynamics.